Evaluation of SMOS Retrievals of Soil Moisture over the Central United States with Currently Available In-situ Observations

Thomas W. Collow and Alan Robock

Department of Environmental Sciences, Rutgers University, New Brunswick, NJ

Jeffrey B. Basara and Bradley G. Illston

Oklahoma Climatological Survey, University of Oklahoma, Norman, OK

Submitted to *Journal of Geophysical Research*

November, 2011

Corresponding Author:
Thomas W. Collow
Department of Environmental Sciences
Rutgers University
14 College Farm Road
New Brunswick, NJ 08901
Phone: 732-932-9800
Fax: 732-932-8644
E-mail: tcollow@eden.rutgers.edu

Abstract

The European Space Agency launched the Soil Moisture Ocean Salinity (SMOS) satellite in November 2009. Using SMOS soil moisture retrievals for 2010 processed using algorithm V4.00, we evaluated SMOS retrievals by comparing them to in-situ soil moisture observations for the top 5 cm at several stations in the Great Plains of the U.S. A major issue with comparing the satellite data with in-situ data is that a SMOS footprint is about 40 km across and we compare to point observations. To address this issue, we chose locations in Oklahoma that have 10 to 25 different in-situ observations within each SMOS footprint. The SMOS retrievals have a dry bias when compared to the average of all in-situ stations in a footprint. Large differences exist between the in-situ observations, even for probes only a few meters apart. Observations from different sensors within a SMOS footprint differ from each other by a larger amount than they differ from the SMOS retrieval. Removing the mean and normalizing the data brings the in-situ observations into better agreement with each other and with SMOS but they still contain substantial differences. Agricultural Research Service Micronet regions in Oklahoma had highly varying values of soil moisture despite being in close proximity to one another, but when averaged and compared to SMOS they had less of a bias than the other regions. Further north in the Great Plains, SMOS retrievals of top 5 cm soil moisture from descending orbits were consistently about 5% by volume wetter than ascending retrievals.

1. Introduction

Soil moisture consists of only 0.01% of the total water on the planet [*Prigent et al.*, 2005]. But soil water content is important for many reasons, such as agriculture. Soil water content also has an important influence on climate, as it determines the partitioning of energy at the surface between sensible and latent heat [*Li et al*., 2007; *ESA*, 2002]. To better understand the interactions of soil moisture with the climate system, an accurate assessment of soil moisture globally must be made. Land surface models have been able to estimate the global soil moisture distribution, but are handicapped by their lack of access to reliable information on soil properties and atmospheric forcing, as well as inaccuracies in the models themselves. It is also difficult to evaluate how well the models simulate the actual soil moisture [*Prigent et al.*, 2005]. In-situ observations only cover a small fraction of the planet, as the cost of direct observation of soil moisture is very high [*Vinnikov et al.*, 1999]. However, a satellite can orbit the entire planet daily and provide routine soil moisture measurements for every location [*Kerr et al.*, 2001], even those that are not inhabited by humans. As in the case of the land surface models, it is difficult to evaluate the remote sensing retrievals of soil moisture. But in locations with in-situ observations it is possible to compare the two different measurements and evaluate the effectiveness of the satellite.

Satellite sensors measure soil moisture at a large spatial resolution while in-situ stations measure soil moisture at a single point [*Jackson et al.*, 2010]. Therefore, locations can only be used as evaluation sites if there are sufficient in-situ stations. It has already been established that there is significant spatial variability of soil moisture. *Entin et al.* [2000] have established a spatial autocorrelation of soil moisture of about 500 km, much greater than any regions being looked at in this study. However, they also suggested that there is a smaller scale of variation

that is dominated by land surface variations. *Crow et al.* [1999] also claimed that there were differences between the coarse scale (> 10 km) and the fine scale (< 1 km) and attributed the fine scale variability to the effects of local variations in topography, soils, and vegetation. However, while the aforementioned studies focused on the stations themselves, here we will attempt to create a mean dataset to evaluate SMOS footprints in different regions only where there are many in-situ stations in a very small area.

Satellite microwave measurements can only sample the top soil layer, typically only a few cm. Microwave observations of soil moisture from satellite radiometers are sensitive to the effects of water on the dielectric constant of the soil, which affects the emissivity [*Jackson and Schmugge,* 1989]. Using satellite data in conjunction with land surface data will allow for a global data set of soil moisture to be assimilated into a model, which may allow for better prediction of precipitation over land [*Reichle et al*., 2004]. Here we evaluate satellite retrievals of top 5 cm soil moisture by using dense networks of in-situ soil moisture observations, using the Soil Moisture Ocean Salinity (SMOS) satellite. The European Space Agency launched SMOS in November 2009. According to *Kerr et al.* [2001], SMOS is designed to have an error less than 0.04 m^3/m^3 and a spatial resolution better than 50 km. *ESA* [2002] projects a resolution between 35 and 50 km. SMOS is not the first satellite to directly measure soil moisture, as other satellites such as the Advanced Microwave Scanning Radiometer (AMSR-E) on board the Aqua satellite and the Scanning Multi-channel Microwave Radiometer (SMMR) have been used. AMSR-E measures soil moisture at a resolution of 60 km at a frequency of 6.92 GHz [*Njoku et al*., 2003] and SMMR measures at a frequency of 6.63 GHz [*Reichle et al*., 2004]. However, frequencies in this range (C-band) are more sensitive to errors resulting from the effects of vegetation and surface roughness, and do not retrieve signals from other than the very top cm or two of the soil.

At lower frequencies (longer wavelengths), this effect is decreased, but too low a frequency will result in interference from anthropogenic radio waves. Frequencies of 1-2 GHz (L-band) are ideal for soil moisture measurements [*Njoku et al*., 2003]. *Vinnikov et al.* [1999] explained that L-band radiometers can penetrate the vegetation canopy of any density and that the retrievals would be primarily a function of soil moisture. SMOS is different from the other satellites, in that it operates at a frequency within this range, 1.4 GHz [*Kerr et al.*, 2001; *ESA*, 2002].

A satellite makes both an ascending and a descending pass each day. In the case of SMOS over the central United States, descending passes occur during the evening between 00 UTC and 01 UTC and ascending passes occur in the early morning between 11 UTC and 12 UTC. This corresponds to the plan made by *Kerr et al.* [2001], which called for a sun synchronous orbit and 6 am ascending passes to coincide with sunrise. During the day, surface drying may create errors as the near surface layer (0-1 cm) may undergo significant drying [*Njoku et al*., 2003] and not be representative of the in-situ soil moisture data which is measured to a depth of 5 cm. Therefore, ascending and descending passes are separated in this study to determine if there is a difference between the two.

2. Data

Several different in-situ sites were used across the central United States. The high density of sites near Stillwater, Oklahoma, was beneficial as not only was there a high number of stations within a single SMOS footprint, but it also enabled an investigation of the in-situ data themselves. The same is true for the two ARS Micronets. Each of the in-situ data sets is described here. Table 1 provides a list of all in-situ stations used, their coordinates, and their elevations.

87 **2.1. United States Climate Reference Network (USCRN)**

88 The United States Climate Reference Network (USCRN) is maintained by the National
89 Climatic Data Center (NCDC) (http://www.ncdc.noaa.gov/crn/). The first USCRN soil moisture
90 sensors were installed in Crossville, Tennessee, in April 2009. Each station consists of three
91 sensors placed at 5, 10, 20, 50, and 100 cm depths. The three sensors are located around the
92 main tower and are only several meters apart [*LeDuc*, 2010]. The sensor used is the Stevens
93 Hydra Probe and its calibration procedures are outlined by *Seyfried et al*. [2005]. The benefit to
94 using three sensors is that soil moisture variations on a very small scale are captured as even the
95 slightest variation in soil texture can change its water content. Also, if one of the sensors
96 malfunctions the other two will continue to provide measurements eliminating the potential for
97 long periods of downtime at any particular station. This study uses hourly observations of soil
98 moisture at 5 cm depth for the 2010 calendar year. Data for every USCRN soil moisture site are
99 available online (http://www1.ncdc.noaa.gov/pub/data/uscrn/products/soilsip01/).

100 **2.2. Soil Climate Analysis Network (SCAN)**

101 The Natural Resources Conservation Service (NRCS) of the United States Department of
102 Agriculture (USDA) operates the SCAN network, which consists of 129 stations located in 39
103 states [*Schaefer et al*., 2007]. SCAN data have been available from the three locations used in
104 this study, Little Washita, OK, Mandan, ND, and Crescent Lake, MN since 1996, 1997, and
105 1998 respectively. Like the USCRN, in this study hourly soil moisture measurements at 5 cm
106 depth for 2010 are used. Each SCAN station has instrumentation to measure soil moisture at
107 depths of 5, 10, 20, 50, and 100 cm depths [*Njoku et al*., 2003] which is identical to the USCRN.
108 The mean station density is one station per 85,000 km^2 [*Jackson et al.*, 2010]. The sensor used is

the Stevens Hydra Probe, as used for USCRN. Data for every SCAN station are available online (http://www.wcc.nrcs.usda.gov/scan/).

2.3. Oklahoma Mesonet

The Oklahoma Mesonet consists over 100 sites measuring 5 cm soil moisture every 30 minutes. The mean density of the soil moisture network is one station per 1677 km^2, which is much higher than SCAN. Soil moisture is also measured at 25, 60, and 75 cm depths but at fewer locations [*Illston et al*., 2008]. To remove extremes of both bare soil and fast growing vegetation, only locations with uniform, low growing vegetation were used as Mesonet station locations [*McPherson et al*., 2007]. The sensor used is the Campbell Scientific 229-L. It is cylinder-shaped and has a length of 60 mm and a diameter of 14 mm [*Illston et al*., 2008]. A ceramic matrix surrounds 32 mm of the cylinder and inside is a thermocouple and a resistor [*Illston et al*., 2008]. The temperature is measured by the thermocouple before and after a 21-second heat pulse is transmitted through the resistor [*Illston et al*., 2008]. The difference between the two measurements provides information on the soil water potential which can be translated to soil water content [*McPherson et al*., 2007] using an empirical relationship developed by *Arya and Paris* [1981], which requires information on the particle size distribution and the bulk density of the soil, both of which are available in soil survey reports . For wet soil the temperature difference will be smaller and for dry soil the difference will be larger [*McPherson et al*., 2007]. Calibration of the sensor is done in a laboratory by attempting to obtain the highest and lowest values of heat dissipation. First the sensor is placed into a bag with desiccant to remove moisture to obtain the largest temperature difference to simulate the driest possible conditions. Then the sensor is placed into a beaker of distilled water and as a result is

saturated, allowing the lowest possible value of dissipation to be measured simulating the wettest possible conditions [*Illston et al*., 2008].

2.4. COsmic-ray Soil Moisture Observing System (COSMOS)

The COSMOS probe measures soil moisture every hour beginning July 21, 2010. The data are different from the other sources in that the sensors are placed above ground and the soil is not disturbed. Measurements of soil moisture on a horizontal scale of about 670 meters and a vertical depth between 12 cm (wet soil) and 76 cm (dry soil) are inferred by measurements of cosmic ray neutrons that are generated within the soil and emitted back to the atmosphere, where they are measured [*Zreda et al*., 2008]. The backscattered flux of slow neutrons is proportional to the density of hydrogen atoms. Since water is the major source of hydrogen atoms that changes with time, the neutron probe can yield a good estimate of soil moisture [*Robock et al*., 2000]. Benefits to this technique are that the footprint comprises a large volume rather than a single point, although the size of the area in the case of COSMOS is still much smaller than the size of the SMOS footprint. Data are available online (http://cosmos.hwr.arizona.edu/).

2.5 Agriculture Research Sevice (ARS) Micronet

The ARS operates two Micronets in southwestern Oklahoma; Little Washita and Fort Cobb. They consist of high density soil moisture measurements every 15 minutes at 5, 25, and 45 cm depths. The Little Washita Micronet consists of 20 stations and the Fort Cobb Micronet has 15 stations. The Little Washita Micronet was first established in the early 1990s and the Fort Cobb Micronet in 2005. *Cosh et al.* [2005] have determined that the average soil moisture from all of the stations in the Micronet is a good representation of the mean soil moisture within the watershed based on results from Soil Moisture Experiment 2003 (SMEX03). The sensor used is the Stevens Hydra Probe, the same as for SCAN and USCRN. Data from the two Micronets as

154 well as information about the individual sites are available for download (http://ars.mesonet.org).
155 Because of the large number of sites, a range of coordinates and elevations was given in Table 1
156 rather than listing them individually for each station. A map of the region encompassing the two
157 Micronets is shown in Figure 3.

158 **2.6 SMOS**

159 The SMOS satellite was launched at the end of 2009 and underwent its commissioning
160 phase through May of 2010. During that time frame and extending into the fall of 2010 many
161 changes were made to the algorithms used to determine soil moisture. To provide a consistent
162 data set for calibration and validation, the 2010 data set was reprocessed with the latest version
163 of the algorithms, which is the V4.00 data being used in this study [*ESLs,* 2011]. The basic
164 mechanism by which SMOS measures soil moisture is through the relationship between
165 microwave emissivity in the L-band (1.4 GHz) and moisture. SMOS measures the brightness
166 temperature, which is a function of the emissivity, and therefore a function of soil moisture. The
167 exact retrieval methods are described in *Kerr et al.* [2011]. A weighting function is applied to
168 SMOS measured brightness temperatures since they are measured at different incidence angles
169 and different incidence angles could affect the results. The values for each pixel are compared to
170 modeled brightness temperatures and a cost function is generated which minimizes the
171 differences between the modeled brightness temperatures and the SMOS weighted brightness
172 temperatures. This is the main component of the soil moisture retrieval algorithm. The actual
173 retrievals are performed on subsets of the weighted pixels, which correspond to soils with low
174 vegetation. The SMOS field of view is not circular, as it has more of a hexagonal shape with
175 concave sides [*Kerr et al.*, 2001]. However this study assumes a circular field of view with a
176 radius of 40 km and a uniform region of influence where the SMOS value is said to be equal

across the entire footprint. This is a simplification due to differences in vegetation and soil type. If two center points are within 40 km of each other, there will be overlap of the footprints.

3. Methods

We created time series for the entire calendar year 2010 using the datasets described above. The location around Stillwater was chosen due to the large number of stations in that region. The Oklahoma Mesonet sites at Stillwater (STIL), Marena (MARE), and Perkins (PERK) were used, as well as USCRN sites Stillwater 2 W and Stillwater 5 WNW and the COSMOS SMAP OK site. Each USCRN site contains three soil moisture sensors, which we plotted individually and the COSMOS data are only available starting July 21. A map of the station locations is shown in Figure 1. Another map showing the close proximity of the USCRN stations, as well as the Mesonet STIL station is shown in Figure 2. The SMOS center point was chosen so that all of the in-situ stations reside within the footprint meaning that each station is no more than 20 km from the center point. The haversine formula was used to calculate the distance between two points and find which points would be acceptable for use. Two SMOS points around Stillwater met the criteria and were used in this study. These two points and their respective footprints are outlined in Figure 1. The points on all the SMOS time series plots are color coded to reflect ascending and descending passes.

In some plots we removed the annual mean soil moisture values for each individual dataset to account for systematic biases (Figure 4). In some plots the data were also normalized by dividing by the standard deviation of each dataset. Scatter plots were created to perform a statistical analysis of the data. To assess SMOS performance, the in-situ datasets were averaged to together to create a mean dataset which represented the approximate in-situ soil moisture of the SMOS footprint which was compared to the values retrieved by SMOS for that footprint

(Figure 5). This same approach was used by *Jackson et al.* [2010] in validation of AMSR-E data. Scatter plots were made for the raw data for both SMOS footprints (Figure 6). Each plot included the correlation coefficient (*r*), the root mean square error (*RMSE*), and the bias (*b*). Bias was calculated by taking the difference between each SMOS and the averaged in-situ measurements and taking the mean. *RMSE* was calculated by taking the difference of each SMOS and the in-situ measurements, squaring them, and then taking the mean. To show the relationship between ascending and descending points, the values of *r*, *RMSE*, and *b* were computed only considering times with in-situ data correspond with ascending or descending passes and represent the different colors on the plots. The aforementioned techniques were also used in analyzing the second SMOS center point.

The variability of the ARS Micronet stations in Fort Cobb, OK and Little Washita, OK was examined. For each watershed, all of the Micronet data were averaged and compared to SMOS. The SMOS center point was chosen so that most, if not all, of the stations would fall into a single footprint. Soil moisture data for 2010 from the individual stations were averaged together to create a mean time series. This was done for both the Little Washita and the Fort Cobb watersheds. SMOS center points were chosen as they were for Stillwater and were chosen to include as many of the Micronet sites as possible. Time series were created for the Little Washita and Fort Cobb watersheds (Figures 7 and 8 respectively) which include a time series of all of the individual Micronet stations as well as the average of all of the stations for the respective watershed. Mesonet sites at Acme (ACME) and Apache (APAC) as well as SCAN site 2023 (Little Washita) all fall within the Little Washita Micronet and were included in the time series. The Mesonet site at Hinton (HINT) is within the Forb Cobb Micronet and is subsequently included in its time series. Scatter plots for the two Micronets were generated in

223 the same manner as for Stillwater showing the same statistical variables (Figure 9). Only the
224 Micronet data was considered for the scatter plots as the SCAN and Mesonet data are only
225 plotted in the time series for a visual reference. The top panel of Figure 9 represents Little
226 Washita and the bottom panel Fort Cobb.

227 Just looking at soil moisture in Oklahoma is not sufficient for a full evaluation. We also
228 examined soil moisture stations located farther north. Because there are only a limited number
229 of in-situ stations, the SMOS evaluation is not complete in this region, but the results reveal
230 certain patterns within the SMOS retrievals themselves. We also examined USCRN site
231 Aberdeen 35 WNW in South Dakota, SCAN site 2002: Crescent Lake, Minnesota, and SCAN
232 site 2020: Mandan, North Dakota. For each station a time series was created for the 5-cm soil
233 moisture in-situ data as well as that for the closest SMOS point (Figure 10 for Aberdeen 35
234 WNW, other stations not shown). Scatter plots were also created for each of the stations and
235 show the same information as those created for Stillwater (Figure 11 for Aberdeen 35 WNW,
236 other stations not shown).

237 To assess the spatial variability further, semi-variograms along with correlation lag plots
238 were created. The semi-variograms were created using the method described in *Liu et al.* [2001]
239 and provide information on the relationship of soil moisture measurements at close distances.
240 The distance between each pair of the three USCRN sensors at one station was assumed to be
241 5 m. The bins were done at 5 km intervals except in the case of Stillwater where the first
242 averaged value represents the mean of the 5 m data only, which represents the individual
243 USCRN sensors at the two stations. This was done to analyze the nugget effect, since this
244 distance is essentially equal to zero when compared to the other distances used, which are on the
245 order of 10^4 m. The points at (0,0) on the semi-variograms and (0,1) on the correlation lag plots

were removed since it is unnecessary to account for the relationship of one station with itself. The semi-variograms and correlation lag plots are shown in Figure 12 with the semi-variograms on the left and the corresponding correlation lag plot to the right of its respective semi-variogram.

4. Results

The time series of the in-situ stations around Stillwater, seen in Figure 4, shows large differences among the soil moisture data from the different stations. It appears that the Oklahoma Mesonet sites have higher mean soil moisture than the other stations with yearly means for STIL, MARE, and PERK of 0.42 m^3/m^3, 0.33 m^3/m^3, and 0.34 m^3/m^3 respectively. The differences between the in-situ stations are as large as the differences between the SMOS retrieval and each in-situ station. Removing the mean (bottom panel of Figure 3) brings the data into closer agreement but large differences still exist, particularly during rapid upward increases in soil moisture after precipitation. For example, sensor 1 from USCRN 5 WNW shows a strong upward increase due to precipitation in the beginning of the year since its yearly mean is so low (0.19 m^3/m^3) compared to other sensors. However, the other sensors do not have values this high. In fact the Mesonet sites have much smaller values because their means were so high. The standard deviation of the USCRN sensors is higher than the others with values ranging between 0.09 m^3/m^3 and 0.12 m^3/m^3. The range of the standard deviation for the Mesonet sensors is between 0.05 m^3/m^3 and 0.07 m^3/m^3. COSMOS has the smallest standard deviation of 0.04 m^3/m^3. When the data are normalized by dividing each mean removed time series by its respective standard deviation (not shown) it appears the variations are in better agreement, but the values themselves are still different and no closer in proximity to just using mean-removed values. The total *RMSE* (ascending and descending combined) for SMOS center point 1 and

SMOS center point 2 is 0.12 m^3/m^3 and 0.13 m^3/m^3 respectively. Upon removing the mean of the data, the *RMSE* values both reduce to 0.06 m^3/m^3. Normalizing results in a *RMSE* of 0.07 m^3/m^3 for the two points.

One important consideration in these comparisons is that the SMOS footprint covers a large area. If there is a rainfall event that produces wet soil in a part of the footprint that has no in-situ stations, large differences could result. As expected, the soil moisture both from in-situ and SMOS appears higher in the winter and early spring than in the middle of the summer because evaporative forcing is higher in the summer. This can be seen in more detail in Table 2. SMOS recorded its highest value of 0.59 m^3/m^3 at two times, 12 UT March 25 and 12 UT April 2, both from center point #1. It was confirmed through looking at archived Next Generation Radar (NEXRAD) images available from NCDC (http://www4.ncdc.noaa.gov/cgi-win/wwcgi.dll?WWNEXRAD~Images2), that precipitation was falling at the times of the two measurements. However, the second footprint retrieved observations of 0.45 m^3/m^3 on the March 25 and 0.41 m^3/m^3 on April 2, which were substantially smaller than that of the first footprint. Based on the radar data it appeared that the rainfall was widespread over the two footprints. The second footprint shows some dry observations in early April that were not present in the first footprint and explains the large difference between the two monthly averages, as seen in Table 2. The average of all the in-situ data is plotted along with the two SMOS footprints in Figure 5. The SMOS footprints are similar but do show some differences such as the case described above. For the most part, the mean of the two SMOS center points falls below the mean of all of the in-situ points, illustrating the overall negative bias. The scatter plots in Figures 6 reveal that the two footprints offer similar statistics, which are expected since there is a large amount of overlap. Both show good correlation between the in-situ and the SMOS but

show a strong negative bias. For these points there is no difference between the ascending and descending passes as biases are still between –0.09 m^3/m^3 and –0.11 m^3/m^3. Stations analyzed farther north show different results.

The Oklahoma Micronet data for the Little Washita and Fort Cobb Micronets were plotted in Figures 7 and 8 respectively. Both show strong variability between the individual stations consistent with the results from Stillwater. The mean spread of the soil moisture values from the Micronets were 0.23 m^3/m^3 and 0.24 m^3/m^3 for Little Washita and Fort Cobb respectively. The spread is defined as the difference between the maximum observed soil moisture value and the minimum soil moisture value at the same time. With such a large spread it is difficult to compare to SMOS observations. The maximum spread of the Little Washita Micronet was 0.50 m^3/m^3, which is extremely large. The lowest spread value computed for both Micronets was 0.11 m^3/m^3, which is larger than the negative SMOS biases measured at Stillwater. When both Micronets were averaged into one time series the mean Micronet values became 0.14 m^3/m^3 and 0.15 m^3/m^3 for Little Washita and Fort Cobb respectively. The Mesonet sites ACME and APAC, within the Little Washita region, registered mean values of soil moisture of 0.33 m^3/m^3 and 0.35 m^3/m^3 respectively. The nearby SCAN site had a mean value of soil moisture of 0.31 m^3/m^3. The HINT Mesonet site near Fort Cobb had a mean soil moisture of 0.32 m^3/m^3. The Mesonet data and SCAN data were not included in the SMOS comparison because their soil moisture values were much higher than those from the Micronets. This can be seen visually in Figures 7 and 8. SMOS was compared only to the mean of the Micronets. There was no bias for Little Washita, which was inconsistent from the results found near Stillwater. At Fort Cobb there was a bias of –0.05 m^3/m^3, which is not as pronounced as for Stillwater but still not within 0.04 m^3/m^3 as desired by SMOS.

315 It is evident from Figure 10 that at USCRN site Aberdeen 35 WNW, there are oscillations
316 between ascending and descending passes with higher soil moisture values occurring for
317 descending passes and lower values for ascending passes. Figure 11 shows the scatter plot for
318 the Aberdeen data. The correlations for ascending and descending passes are almost equal
319 (about 0.70), but when combined decrease to 0.63. The negative bias for the ascending passes is
320 larger than for the descending passes. This contradicts the supposition that soil moisture should
321 be at its driest in the late afternoon as SMOS registers the opposite. The same results were seen
322 for the data at two other sites, SCAN 2020 Crescent Lake and SCAN 2092 Mandan. SCAN
323 2020 recorded a descending bias of -0.08 m^3/m^3 and an ascending bias of -0.11 m^3/m^3. SCAN
324 2092 had a descending bias of -0.20 m^3/m^3 and an ascending bias of -0.26 m^3/m^3. For all of the
325 northern sites, an additional SMOS center point was chosen and similar results were found
326 indicating that these findings are not the result of an isolated error. These results are because of
327 radio frequency interference from the North Warning System radars across northern Canada
328 (formerly called the Distance Early Warning (DEW) Line), which that preferentially affect the
329 ascending retrievals because of the SMOS antenna pattern [Yann Kerr, personal communication,
330 October 29, 2011]. The radar emissions raise the brightness temperature, artificially lowering
331 the retrieved soil moisture. There is no seasonal cycle of the difference between the ascending
332 and descending retrievals, as the oscillations appear to occur throughout the year, further
333 suggesting the above hypothesis is correct.

334 The semi-variograms in Figure 12 all show a constant sill which is reached very quickly.
335 For the two Micronet regions, the sill is nearly constant at every distance, which shows that there
336 is little relationship between these points even at such close distances. A nugget effect or range
337 cannot be seen at either Micronet region, perhaps as a result of there being no data available to

338 diagnose them. Based on this alone it appears as if there is no spatial relationship with the
339 Micronet data. However, correlation lag plots show correlations generally between 0.5 and 0.9
340 for both Micronets. While this is not perfect it shows that there is at least some spatial
341 relationship between the values. That the mean line is nearly constant shows that the relationship
342 does not depend on distance at such a close range, so theoretically the relationship between two
343 stations 10 km apart would be the same as two stations 30 km apart. Because the data are related
344 in this way, it was valid to use them for SMOS comparisons. Because data are available from
345 individual USCRN sensors it is possible to analyze the semi-variance at near zero distance.
346 Intuitively this value should be near zero, and in fact it is lower than the sill value for Stillwater.
347 When connected to the mean bins for Stillwater, a range is seen in the first few km, which is
348 consistent with fine scale variability described by *Crow et al.* [1999]. Beyond this range, the
349 pattern is similar to the two Micronets as the semi-variograms and correlation lag plots remain
350 constant showing that at this scale the relationship between soil moisture measurements has little
351 dependence on distance.

352 **5. Discussion**

353 The large discrepancy that was found with the in-situ observations presents a major
354 challenge in the evaluation of SMOS. Large differences are due to the known spatial variability
355 of soil moisture, which is influenced by soil type, vegetation, and precipitation, as well as the
356 fact that different instruments and measuring techniques are used. For example, the Little
357 Washita Micronet has soil types that range from a fine sand to a silty loam and SCAN site 2023,
358 which is within that region, has a silty clay soil. Because soil type affects how water infiltrates
359 the soil surface, it is expected that there would be different values of soil moisture at each
360 station. Although the individual values are different, semi-variogram analysis shows that there is

361 almost a constant relationship between the stations that neither improves or degrades with
362 increasing distance, meaning that although the actual values may the different, the trends are
363 similar. Previous work by *Crow et al.* [1999] and *Entin et al.* [2000] describe two scales of soil
364 moisture, but it is possible there could be a third, intermediate scale where the relationship
365 between soil moisture and distance is constant. Studies that attempt to assimilate SMOS data
366 into numerical weather models will face uncertainty in that it will be difficult to assess whether
367 or not the SMOS data being put into the model are accurate enough. It also must be taken into
368 account that SMOS evaluation is not possible when there is snow cover. In the case of
369 Stillwater, according to National Operational Hydrological Remote Sensing Center snow cover
370 analyses, most of Oklahoma was covered in snow during January and February 2010. Although
371 according to Table 2, the monthly average departures between SMOS and in-situ were among
372 the highest, there was most likely error on both sides and not representative of the SMOS
373 evaluation for the rest of the year. In places further north, snow cover is more persistent leading
374 to an even greater time period without proper evaluation. For the USCRN site in Aberdeen, in-
375 situ data are missing for January, February, March, and December (Figure 7).

376 In the case of the extreme values of SMOS, it is uncertain as to whether or not the
377 satellite was recording extra water that did not infiltrate the soil, making the value higher than it
378 otherwise would be. Based on the Figure 4 precipitation plot, there were times during the year,
379 particularly on May 19 and June 14 where precipitation was higher than it was on March 25 and
380 April 2. However, SMOS provided undefined values for those days, making it impossible to
381 determine the relationship with the precipitation. It should also be noted that precipitation has a
382 high spatial variability and will not be uniform over an area even as small as that in Figure 2.
383 Therefore, it will be difficult to determine the exact relationship between SMOS and

384 precipitation, but one would intuitively expect that precipitation should lead to an increase in
385 SMOS values.

386 The reduction in the *RMSE* from the two footprints near Stillwater that resulted from
387 removing the means shows that it might be better to evaluate SMOS after removing all of the
388 station biases as well as the bias of the SMOS point. This shows that SMOS is better at
389 observing trends in soil moisture rather than instantaneous values. However the *RMSE* is still
390 greater than the required accuracy of 0.04 m^3/m^3. More work will need to be done investigating
391 the sites to the north and the reasoning for the oscillations between the ascending and descending
392 passes.

393 The radio frequency interference we found in the northern part of our domain will affect
394 broad regions of the world, and with a larger amplitude as other regions have even larger surface
395 microwave emissions. This further add to the errors in SMOS retrievals, but if the emissions are
396 relatively constant, perhaps useful corrections can be made.

397 Although the negative biases for SCAN 2020 were much larger than the other sites, it
398 cannot be determined whether or not this is from SMOS or the result of an over-estimation of in-
399 situ soil moisture. This is another example of why it is difficult to evaluate SMOS.

400 **6. Conclusions**

401 At present time SMOS evaluation is difficult, due to the lack of uniform soil moisture
402 measurements within a single footprint. Differences were apparent between the three sensors at
403 the USCRN stations that are only several meters apart as well as within the high density
404 Micronet networks.

405 To perform a better evaluation, additional monitoring sites need to be established at other
406 locations and soil moisture data must be made available in an effort to assist with evaluation and

calibration of SMOS and eventually the Soil Moisture Active Passive (SMAP) mission, which will be launched by NASA in 2014. Campaigns such as the Global Soil Moisture Data Bank [*Robock et al.*, 2000] and the International Soil Moisture Network [*Dorigo et al.*, 2011] have already made this possible.

With the present set of in-situ data it can be concluded that the reprocessed SMOS soil moisture data has a dry bias, which places the data below their specified accuracy range. In all but one of the analyses, SMOS came back with a dry bias below that range. Removing the mean and normalizing the data to remove the bias still results in high *RMSE* values relative to the desired error range. Further studies will need to be conducted at additional sites to see if this holds.

Acknowledgments. This work is supported by NASA grant NNX09AJ99G and is conducted as part of the SMOS Validation and Retrieval Team activities. We thank Yann Kerr for the reprocessed SMOS data and for valuable comments on the manuscript, Michael Palecki for the USCRN data, Marek Zreda for the COSMOS data, and Eric Wood for providing us with the reprocessed SMOS data for 2010.

References

Arya, L. M., and J. F. Paris (1981), A physicoempirical model to predict the soil moisture characteristic from particle-size distribution and bulk density data, *Soil Sci. Soc. Amer. J.*, *45*, 1023–1030.

Cosh, M. H., T. J. Jackson, P. Starks, and G. Heathman (2005), Temporal stability of surface soil moisture in the Little Washita River watershed and its applications in satellite soil moisture product validation, *J. Hydrology*, *323*, 168-177.

Crow, W. T., and E. F. Wood (1999), Multi-scale dynamics of soil moisture variability observed during SGP'97, *Geophys. Res. Lett.*, *26*, 3485-3488.

Dorigo, W. A., W. Wagner, R. Hohensinn, S. Hahn, C. Paulik, A. Xaver, A. Gruber, M. Drusch, S. Mecklenburg, P. van Oevelen, A. Robock, and T. Jackson (2011), The International Soil Moisture Network: A data hosting facility for global in-situ soil moisture measurements, *Hydrol. Earth Syst. Sci.*, *15*, 1675-1698, doi:10.5194/hess-15-1675-2011.

Entin, J. K., A. Robock, K. Y. Vinnikov, S. E. Hollinger, S. Liu, and A. Namkhai (2000). Temporal and spatial scales of observed soil moisture variations in the extratropics, *J. Geophys. Res.*, *105*, 11865-11877.

ESA (2002), SMOS Mission objectives and scientific requirements of the Soil Moisture Ocean Salinity (SMOS) mission. Version 5. Available at http://esamultimedia.esa.int/docs/SMOS_MRD_V5.pdf.

ESLs and ARRAY (2011), Release of SMOS level 2 reprocessed soil moisture products. Available at http://calvalportal.ceos.org/cvp/c/document_library/get_file?uuid=98ef88d1-c266-41d0-9a36-55a666814b88&groupId=10136.

445 Illston, B. G., J. B. Basara, C. A. Fiebrich, K. C. Crawford, E. Hunt, D. K. Fisher, R. Elliott, and
446 K. Humes (2008), Mesoscale monitoring of soil moisture across a statewide network. *J.*
447 *Atmos. Oceanic Technol.*, *25*, 167–182, doi: 10.1175/2007JTECHA993.1.
448 Jackson, T. J. and T. J. Schmugge (1989), Passive microwave remote sensing system for soil
449 moisture: some supporting research. *IEEE Trans. Geosci. Remote Sens.*, *27*, 225-235.
450 Jackson, T. J., M. H. Cosh, R. Bindlish, P. J. Starks, D. D. Bosch, M. Seyfried, D. C. Goodrich,
451 M. S. Moran, and J. Du (2010), Validation of advanced microwave scanning radiometer soil
452 moisture products. *IEEE Trans. Geosci. Remote Sens.*, *48*, 4256-4272.
453 Kerr Y. H., P. Waldteufel, J.-P. Wigneron, J.-M. Martinuzzi, J. Font, and M. Berger (2001), Soil
454 moisture retrieval from space: The Soil Moisture and Ocean Salinity (SMOS) mission, *IEEE*
455 *Trans. Geosci. Remote Sens.*, *39*, 1729-1735.
456 Kerr Y. H., P. Waldteufel, P. Richuame, J.-P. Wigneron, P. Ferrazzoli, A. Mahmoodi, A. Al
457 Bitar, F. Cabot, C. Gruhier, S. Juglea, D. Leroux, A. Mialon, and S. Delwart (2011), The
458 SMOS soil moisture retrieval algorithm, *IEEE Trans. Geosci. Remote Sens.*, submitted
459 LeDuc, S., H. J. Diamond, and M. A. Palecki (2010), US Climate Reference Network annual
460 report fiscal year 2010. Available at http://www1.ncdc.noaa.gov/pub/data /uscrn/
461 publications/annual_reports/FY10_USCRN_Annual_Report.pdf.
462 Li, H., A. Robock, and M. Wild (2007), Evaluation of Intergovernmental Panel on Climate
463 Change Fourth Assessment soil moisture simulations for the second half of the twentieth
464 century, *J. Geophys. Res.*, *112*, D06106, doi:10.1029/2006JD007455.
465 Liu, S., X. Mo, H. Li, G. Peng, and A. Robock (2001), Spatial variation of soil moisture in
466 China: Geostatistical characterization, *J. Meteorol. Soc. Japan*, *79*, 555-574.

McPherson, R. A., et al. **(**2007), Statewide monitoring of the mesoscale environment: A technical update on the Oklahoma Mesonet, *J. Atmos. Oceanic Technol., 24*, 301-321.

Njoku, E. G., T. J. Jackson, V. Lakshmi, T. K. Chan, and S. V. Nghiem (2003), Soil moisture retrieval from AMSR-E. *IEEE Trans. Geosci. Remote Sens., 41*, 215-229.

Prigent, C., F. Aires, W. B. Rossow, and A. Robock (2005), Sensitivity of satellite microwave and infrared observations to soil moisture at a global scale: relationship of satellite observations to in-situ soil moisture measurements, *J. Geophys. Res*., *110*, D07110, doi:10.1029/2004JD005087.

Reichle, R. H., R. D. Koster, J. Dong, and A. A. Berg (2004), Global Soil Moisture from Satellite Observations, Land Surface Models, and Ground Data: Implications for Data Assimilation, *J. Hydrometeor*, *5*, 430–442.

Robock, A., K. Y. Vinnikov, G. Srinivasan, J. K. Entin, S. E. Hollinger, N. A. Speranskaya, S. Liu, and A. Namkhai (2000), The Global Soil Moisture Data Bank, *Bull. Amer. Meteorol. Soc.*, *81*, 1281-1299.

Schaefer, G. L., M. H. Cosh, and T. J. Jackson (2007), The USDA Natural Resources Conservation Service Soil Climate Analysis Network (SCAN), *J. Atmos. Oceanic Technol.*, *24*, 2073-2077.

Seyfried, M. S., L. E. Grant, E. Du., and K. Humes (2005), Dielectric loss and calibration of the Hydra Probe soil water sensor, *Vadose Zone J.*, *4*, 1070-1079.

Vinnikov, K. Y., A. Robock, S. Qiu, J. K. Entin, M. Owe, B. J. Choudhury, S. E. Hollinger, and E. G. Njoku (1999), Satellite remote sensing of soil moisture in Illinois, USA, *J. Geophys. Res.*, *104*, 4145-4168.

Zreda, M., D. Desilets, T. P. A. Ferre, and R. L. Scott (2008), Measuring soil moisture content non-invasively at intermediate spatial scale using cosmic-ray neutrons. *Geophys. Res. Lett.*, **35**, L21402, doi: 10.1029/2008GL035655.

Table1. List of all in-situ stations used in this study

Station	Latitude (°N)	Longitude (°W)	Elevation (m)
Stillwater, OK Region			
USCRN Stillwater, OK 5 WNW	36.13	97.11	277
USCRN Stillwater, OK 2 W	36.12	97.09	277
Mesonet STIL	36.12	97.10	272
Mesonet MARE	36.06	97.21	327
Mesonet PERK	36.00	97.05	292
COSMOS SMAP OK	36.06	97.22	326
Little Washita Micronet Region			
Little Washita Micronet (20 stations)	34.79 – 34.98	97.89 – 98.26	343 – 458
SCAN 2023 Little Washita, OK	34.95	97.98	358
Mesonet ACME	34.81	98.02	397
Mesonet APAC	34.91	98.29	440
Fort Cobb Micronet Region			
Fort Cobb Micronet (15 stations)	35.22 – 35.46	98.43 – 98.71	430 – 524
Mesonet HINT	35.48	98.48	493
Northern Stations			
USCRN Aberdeen, SD 35 WNW	45.71	99.13	606
SCAN 2002 Crescent Lake, MN	45.42	93.95	299
SCAN 2020 Mandan, ND	46.77	100.92	588

Table2. Monthly averaged values for 2010 of top 5-cm soil moisture (m^3/m^3) derived from the in-situ mean and the two SMOS footprints around Stillwater (Figure 1). The averaged monthly SMOS biases (as compared to in-situ mean) are also given for each footprint. SMOS diff is the difference between the two SMOS retrievals (SMOS #1 minus SMOS #2).

Month	In-situ mean	SMOS #1	Bias #1	SMOS #2	Bias #2	SMOS diff
Jan	0.39	0.25	-0.14	0.25	-0.14	0.00
Feb	0.41	0.26	-0.15	0.26	-0.15	0.00
Mar	0.39	0.31	-0.08	0.28	-0.11	0.03
Apr	0.35	0.26	-0.09	0.20	-0.15	0.06
May	0.31	0.21	-0.10	0.20	-0.11	0.01
Jun	0.33	0.21	-0.12	0.22	-0.11	-0.01
Jul	0.26	0.13	-0.13	0.14	-0.12	-0.01
Aug	0.20	0.12	-0.08	0.12	-0.08	0.00
Sep	0.23	0.14	-0.09	0.13	-0.10	0.01
Oct	0.21	0.13	-0.08	0.12	-0.09	0.01
Nov	0.28	0.17	-0.11	0.14	-0.14	0.03
Dec	0.24	0.13	-0.11	0.13	-0.11	0.00

Figure Captions

Figure 1. Map of all in-situ soil moisture observing sites near Stillwater, OK used in the analysis. The blue circles represent the SMOS footprints and have radii of 20 km from the SMOS center points. Counties are also labeled.

Figure 2. Google Earth image close-up view of three in-situ soil moisture stations in close proximity of each other near Stillwater, OK. 1000 m scale is in lower left.

Figure 3. Map of all in-situ soil moisture observing sites within the two ARS Micronet regions, Fort Cobb and Little Washita. The blue circles represent the SMOS footprints and have radii of 20 km from the SMOS center points. Counties are also labeled.

Figure 4. Daily precipitation measured from various instruments near Stillwater, OK (top); Raw soil moisture data at locations around Stillwater (middle); Soil moisture data with the means of each individual station removed (bottom).

Figure 5. Top: Time series of the two SMOS center points used near Stillwater, OK. Red dots represent ascending retrievals and blue dots signify descending retrievals. Bottom: time series of the mean of the in-situ data shown in Figure 3 and the mean of the two SMOS footprints.

Figure 6. Top: Scatter plot of soil moisture retrievals from SMOS center point #1 and the mean of the in-situ data used in Figure 3. Points are separated into ascending and descending values and bias, RMSE, and the correlation coefficient are listed in the top left corner for the ascending and descending data as well as the entire dataset combined. Bottom: Same as top but for SMOS center point #2.

Figure 7. Raw soil moisture data measured from the ARS Micronet sites in the Little Washita, OK watershed as well as other sites within the same SMOS footprint. The green line is the mean of all of the Micronet sites.

Figure 8. Same as Figure 7 but for the Fort Cobb, OK watershed.

Figure 9. Top: Scatter-plot of soil moisture retrievals from the SMOS footprint encompassing the Little Washita watershed and the mean of the Little Washita Micronet soil moisture data shown in figure 7. Points are separated into ascending and descending values and bias, RMSE, and the correlation coefficient are listed in the top left corner for the ascending and descending data as well as the entire dataset combined. Bottom: Same as top but for the Fort Cobb Micronet data shown in Figure 8.

Figure 10. Time series of precipitation and soil moisture measured at USCRN site – Aberdeen, SD 35 WNW. Data from the nearest SMOS center point are also plotted.

Figure 11. Scatter-plot of soil moisture retrievals from the SMOS center point near Aberdeen and the mean of the in-situ data used in Figure 10. Points are separated into ascending and descending values. The mean biases and the correlation coefficients for ascending and descending passes are listed in the top left corner.

Figure 12. Semi-variograms (left) and correlation lag plots (right) for the soil moisture stations near Stillwater (top), the Little Washita Micronet (middle), and the Fort Cobb Micronet (bottom).

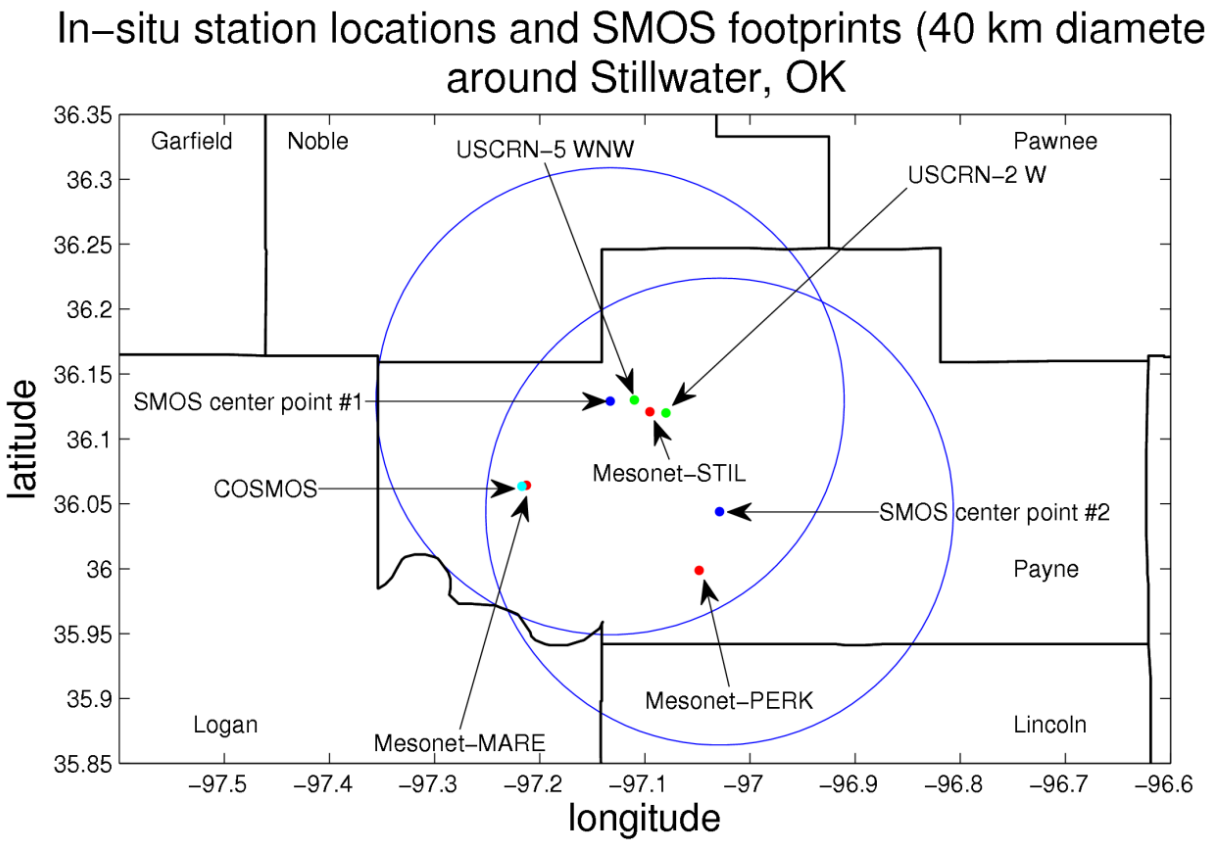

Figure 1. Map of all in-situ soil moisture observing sites near Stillwater, OK used in the analysis. The blue circles represent the SMOS footprints and have radii of 20 km from the SMOS center points. Counties are also labeled.

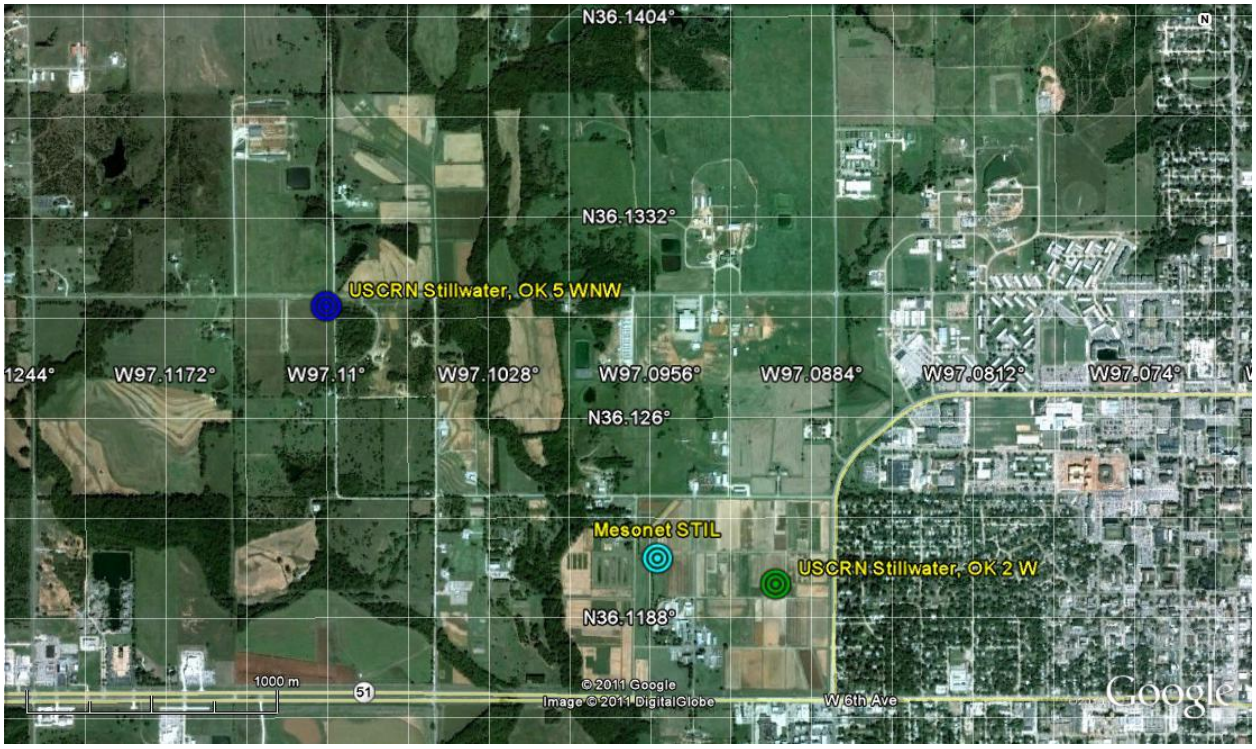

Figure 2. Google Earth image close-up view of three in-situ soil moisture stations in close proximity of each other near Stillwater, OK. 1000 m scale is in lower left.

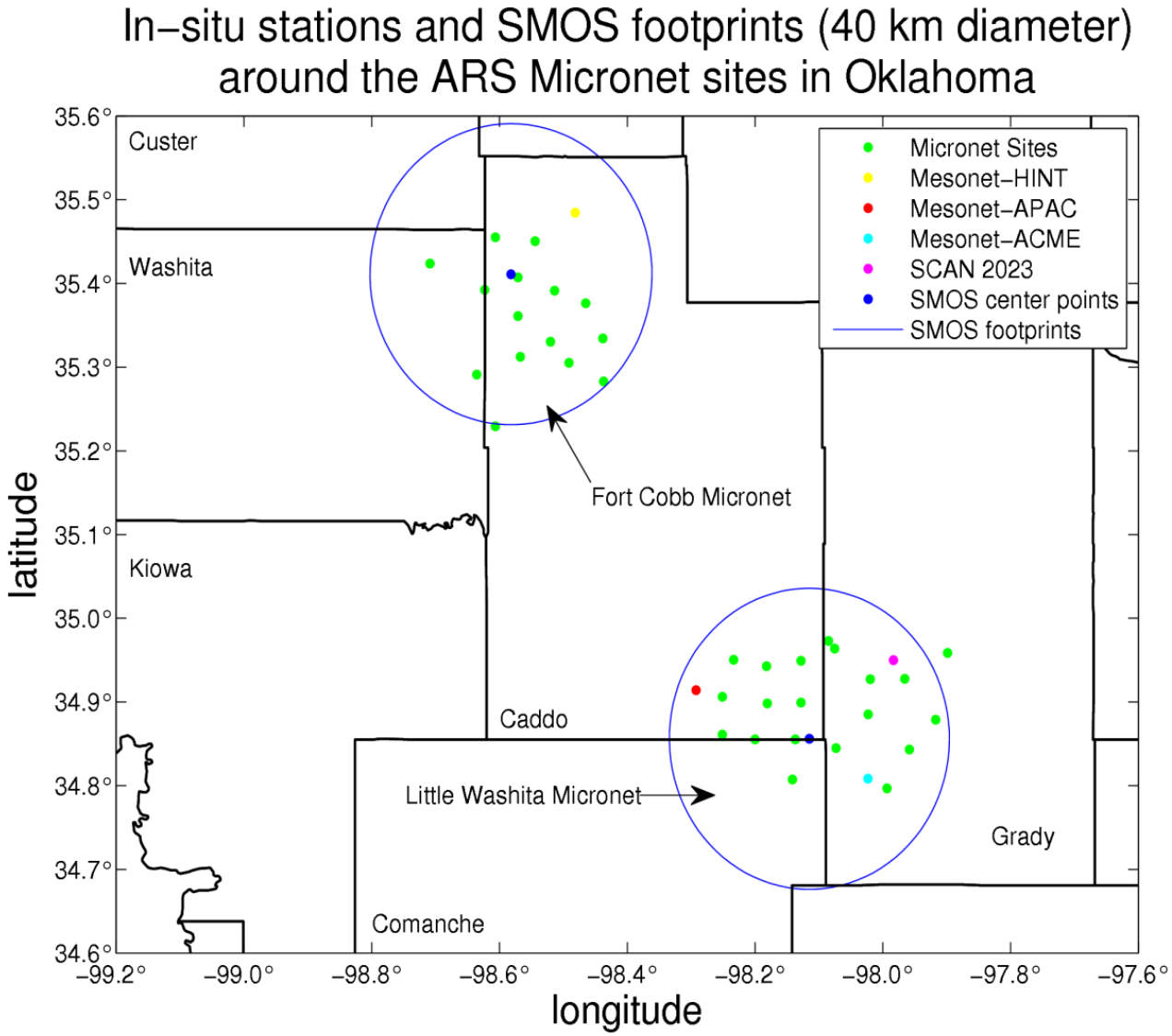

Figure 3. Map of all in-situ soil moisture observing sites within the two ARS Micronet regions, Fort Cobb and Little Washita. The blue circles represent the SMOS footprints and have radii of 20 km from the SMOS center points. Counties are also labeled.

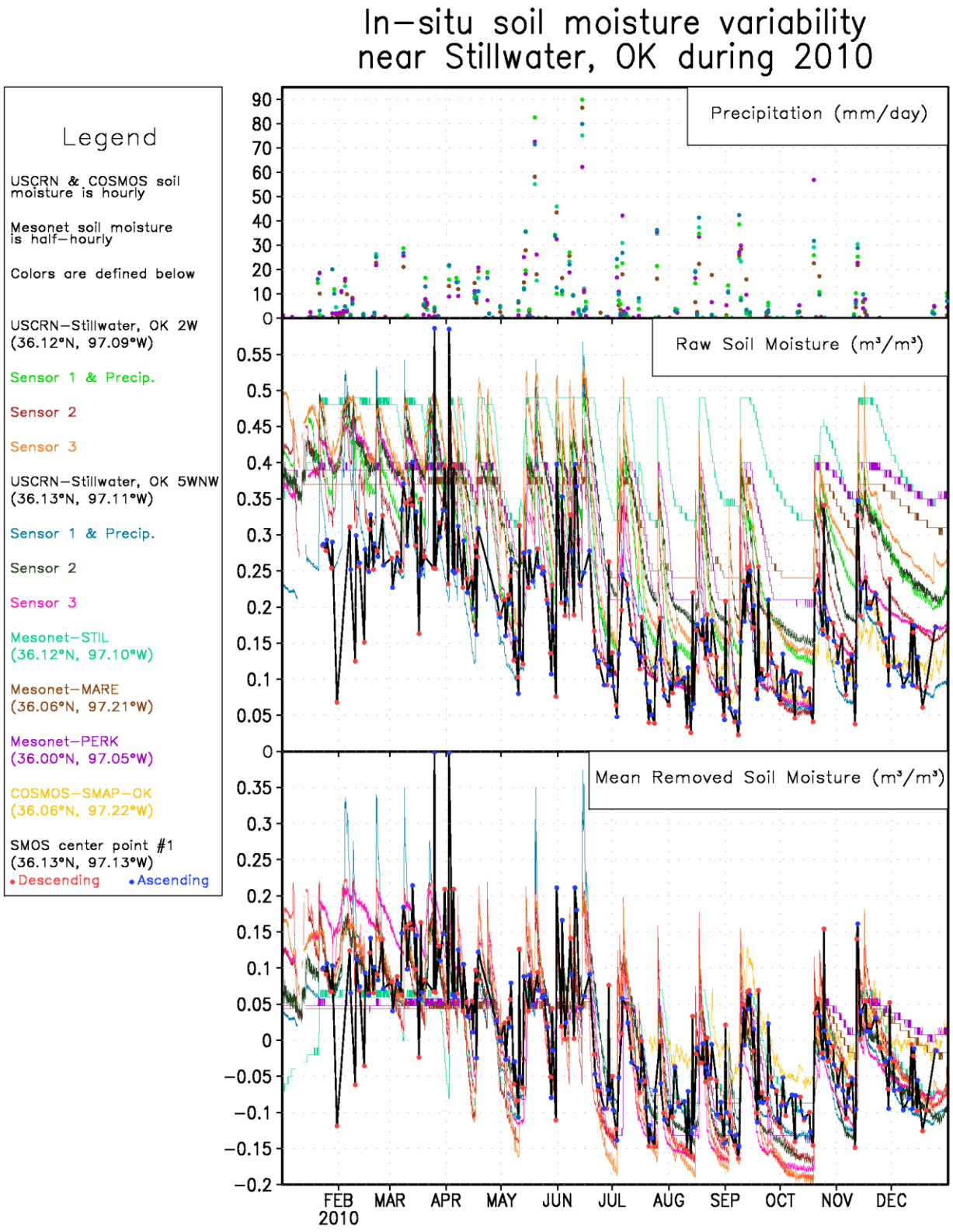

Figure 4. Daily precipitation measured from various instruments near Stillwater, OK (top); Raw soil moisture data at locations around Stillwater (middle); Soil moisture data with the means of each individual station removed (bottom).

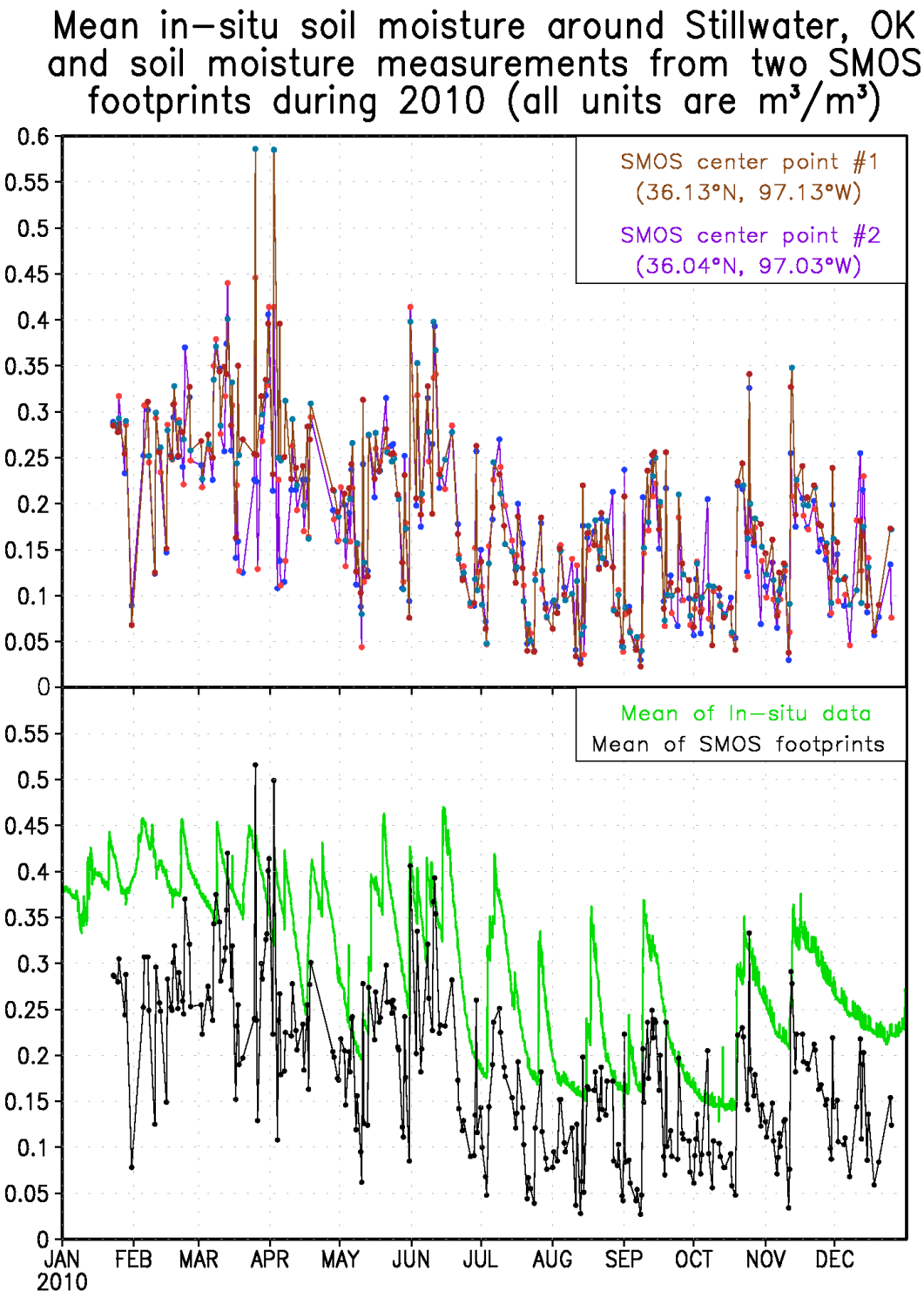

Figure 5. Time series of the two SMOS center points used near Stillwater, OK. Red dots represent ascending retrievals and blue dots signify descending retrievals (top). Time series of the mean of the in-situ data shown in Figure 3 and the mean of the two SMOS footprints (bottom).

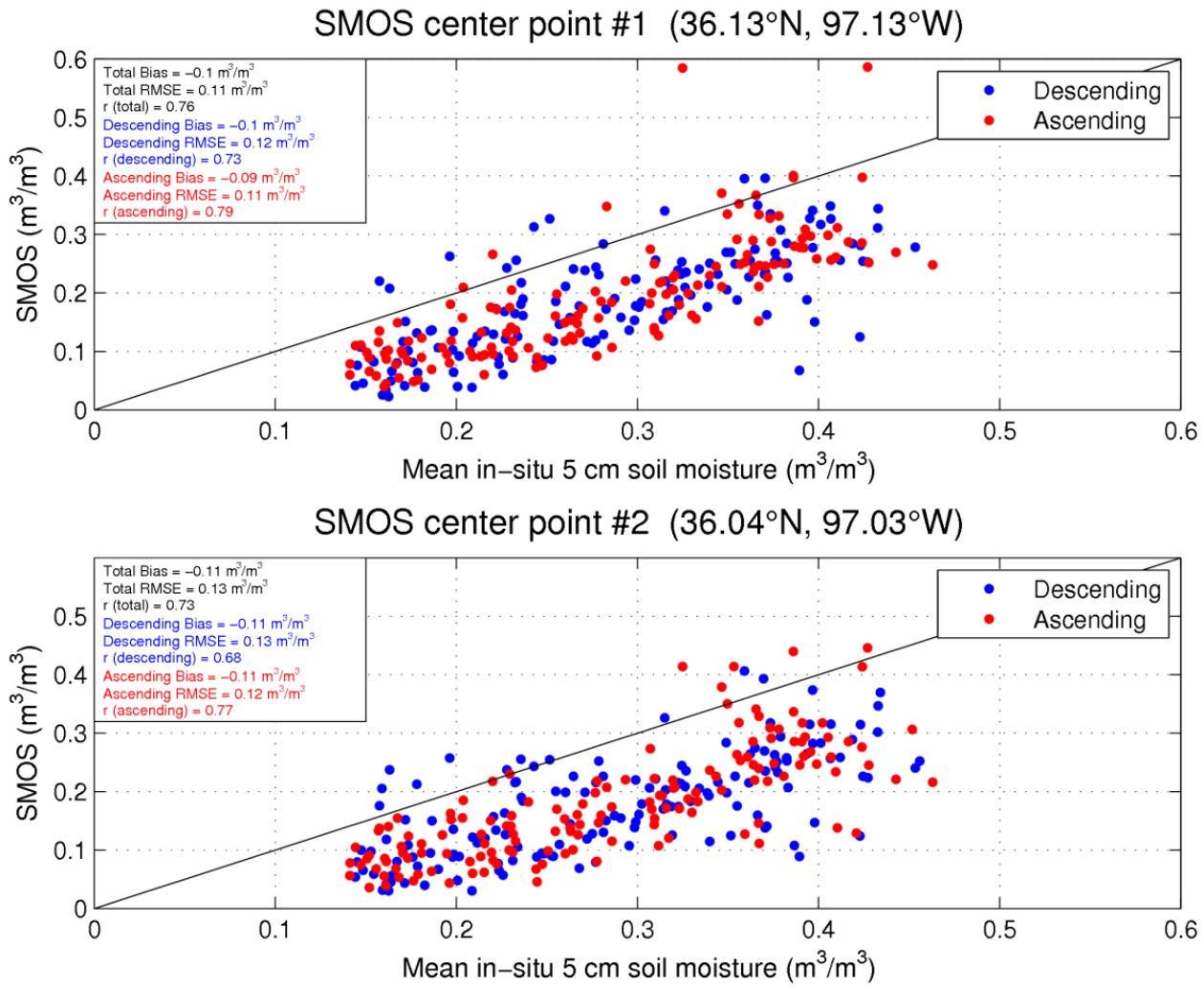

Figure 6. Top: Scatter plot of soil moisture retrievals from SMOS center point #1 and the mean of the in-situ data used in Figure 3. Points are separated into ascending and descending values and bias, RMSE, and the correlation coefficient are listed in the top left corner for the ascending and descending data as well as the entire dataset combined. Bottom: Same as top but for SMOS center point #2.

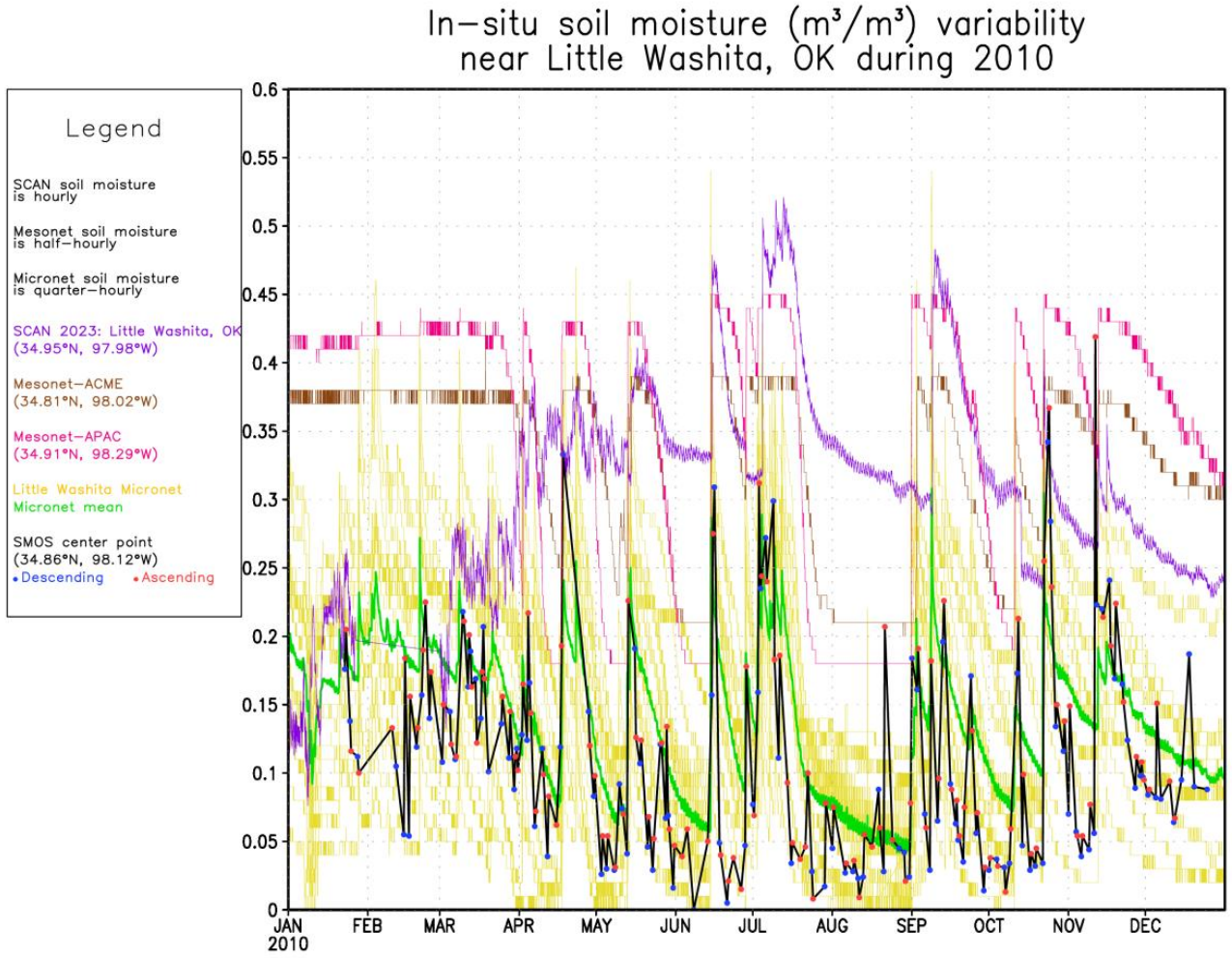

Figure 7. Raw soil moisture data measured from the ARS Micronet sites in the Little Washita, OK watershed as well as other sites within the same SMOS footprint. The green line is the mean of all of the Micronet sites.

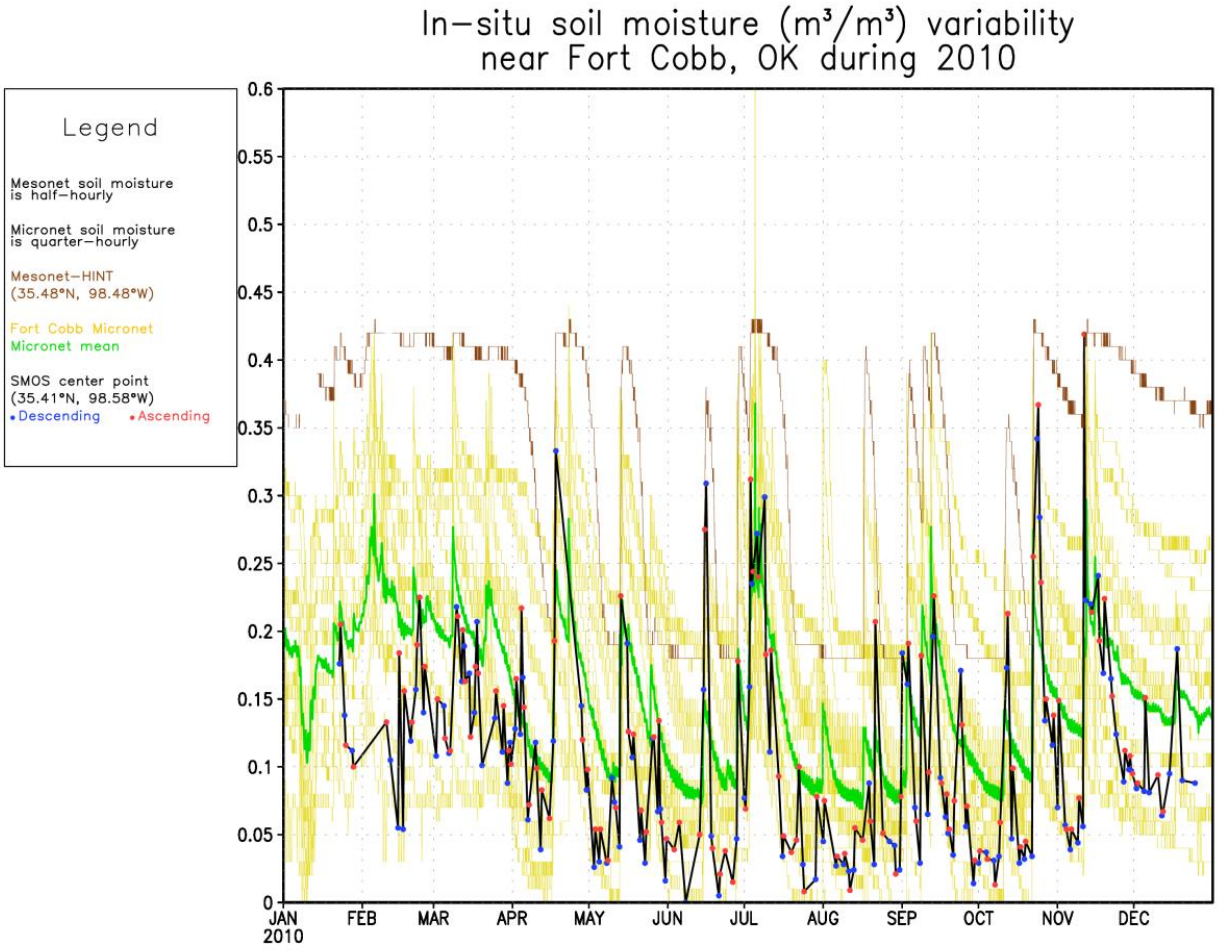

Figure 8. Same as Figure 7 but for the Fort Cobb, OK watershed.

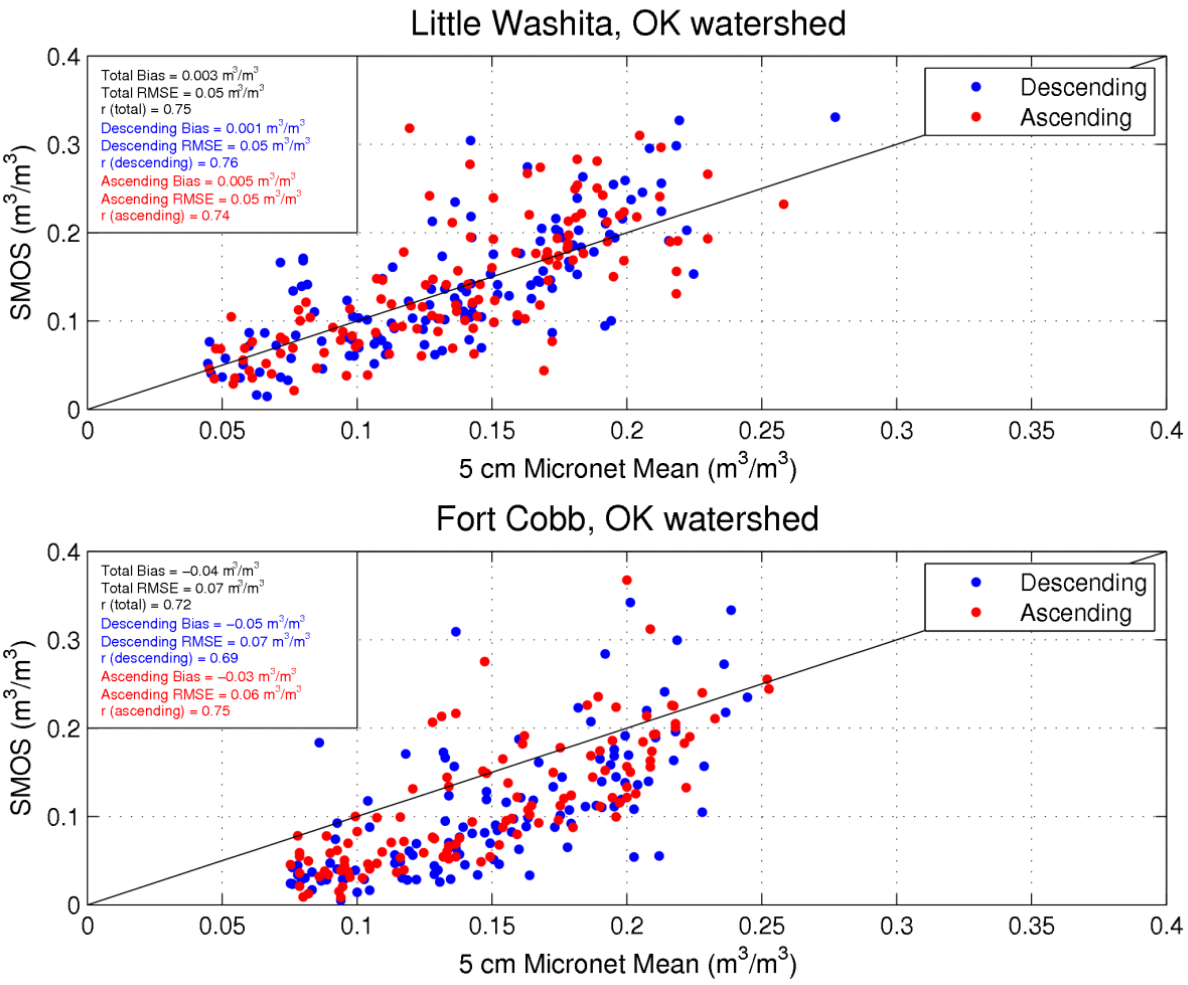

Figure 9. Top: Scatter-plot of soil moisture retrievals from the SMOS footprint encompassing the Little Washita watershed and the mean of the Little Washita Micronet soil moisture data shown in Figure 7. Points are separated into ascending and descending values and bias, RMSE, and the correlation coefficient are listed in the top left corner for the ascending and descending data as well as the entire dataset combined. Bottom: Same as top but for the Fort Cobb Micronet data shown in Figure 8.

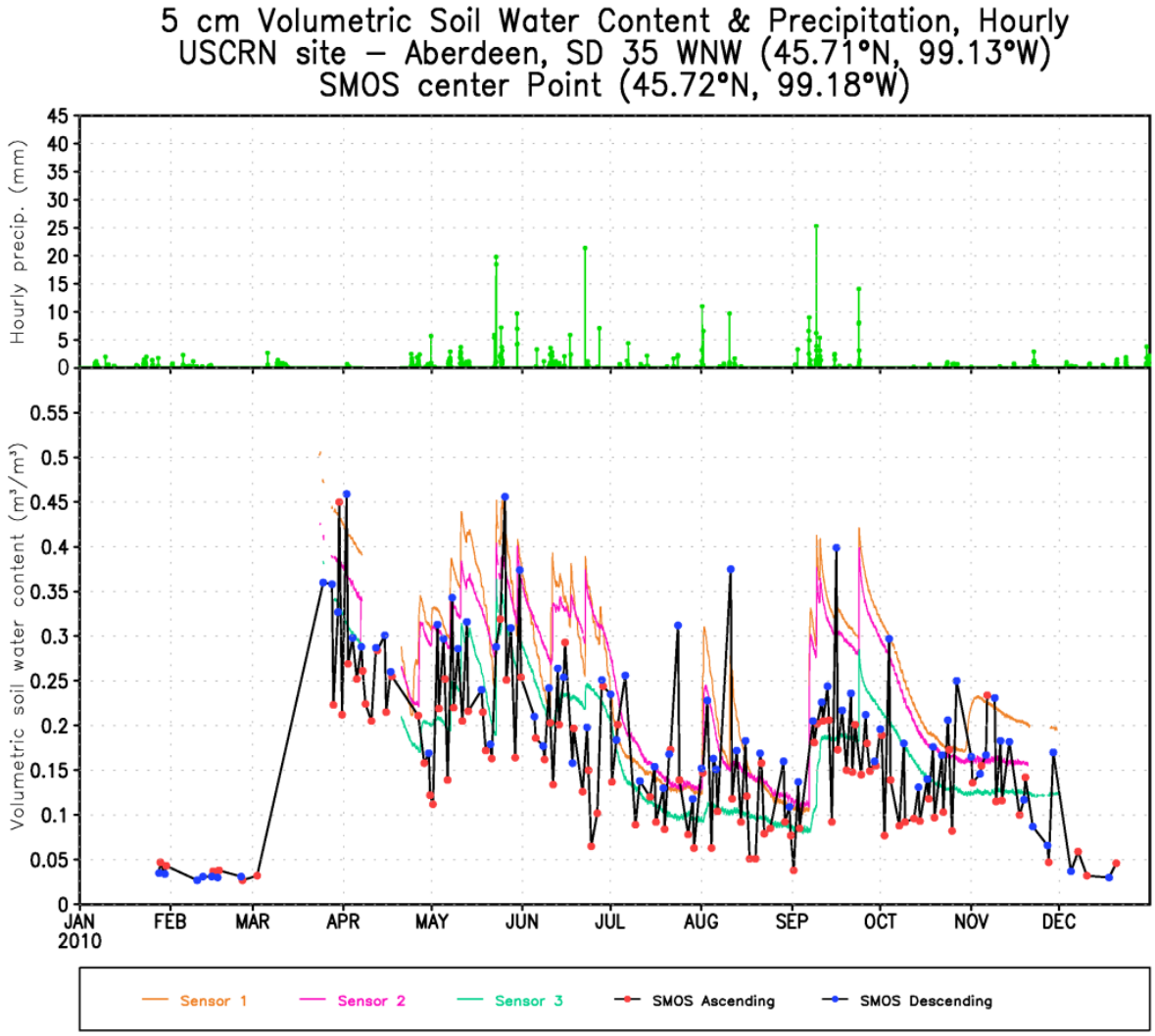

Figure 10. Time series of precipitation and soil moisture measured at USCRN site – Aberdeen, SD 35 WNW. Data from the nearest SMOS center point are also plotted.

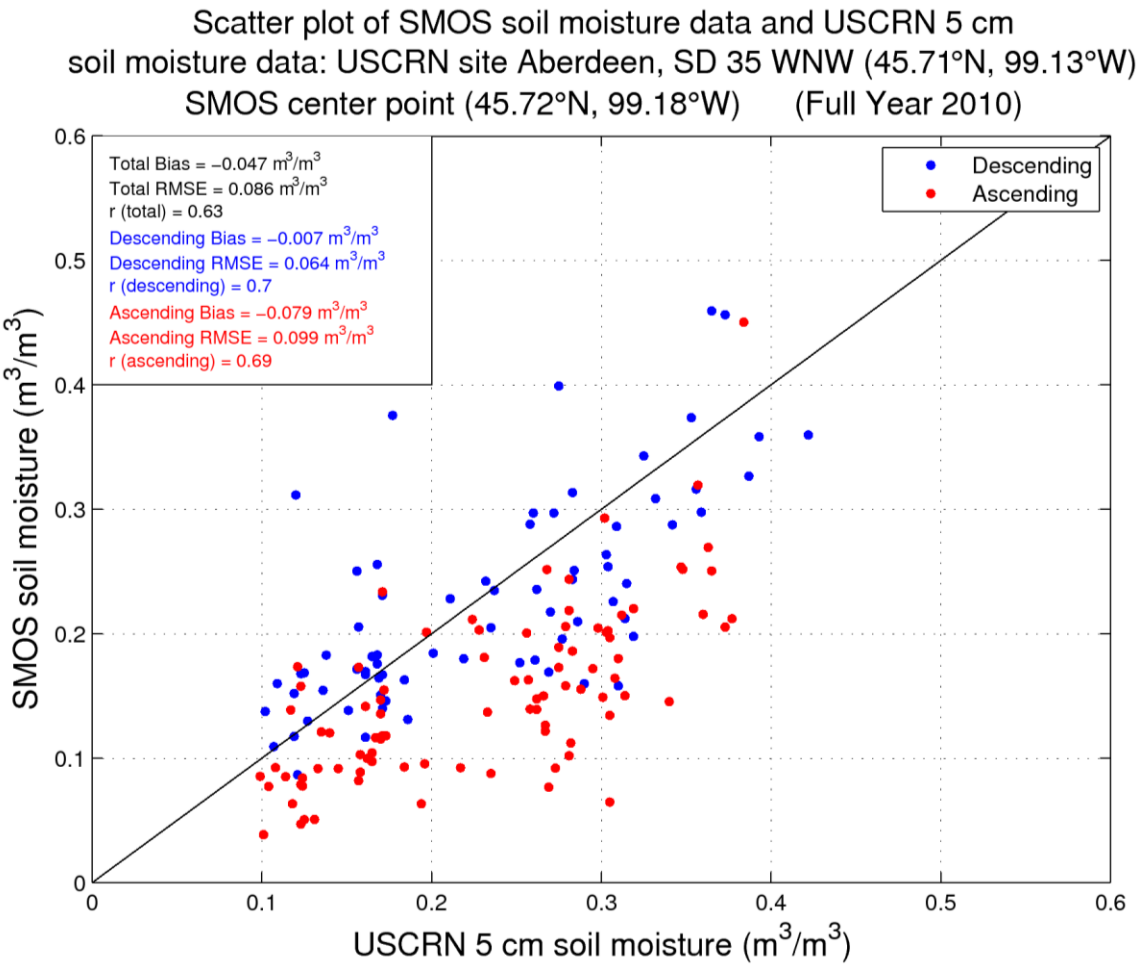

Figure 11. Scatter-plot of soil moisture retrievals from the SMOS center point near Aberdeen and the mean of the in-situ data used in Figure 7. Points are separated into ascending and descending values. The mean biases and the correlation coefficients for ascending and descending passes are listed in the top left corner.

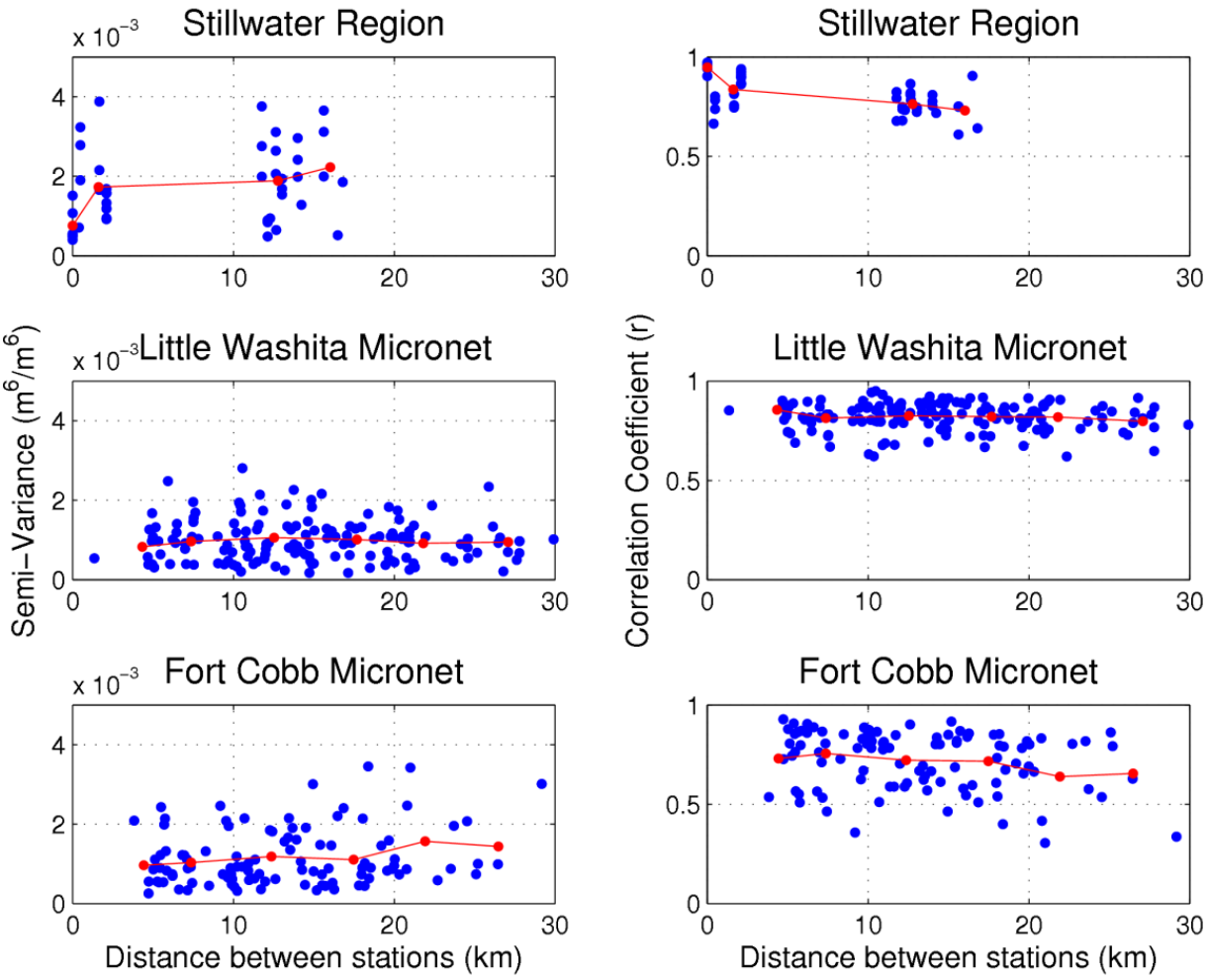

Figure 12. Semi-variograms (left) and correlation lag plots (right) for the soil moisture stations near Stillwater (top), the Little Washita Micronet (middle), and the Fort Cobb Micronet (bottom).